

Optimization of Activation Detector for Benchmark Experiment of Large-angle Elastic Scattering Reaction Cross Section by 14MeV Neutrons

Ryohei TAKEHARA, Kazuki FUKUI, Sota ARAKI, Shingo TAMAKI, Sachie KUSAKA and
Isao-MURATA

Graduate school of Engineering, Osaka University, Yamada-oka 2-1, Suita, Osaka 565-0871, Japan
Email: takehara.ryohei@eb.see.eng.osaka-u.ac.jp

The neutron elastic scattering reaction cross section data commonly show smaller in backward angles compared to those of forward angles when the energy of incident neutron is high. However, in a high neutron flux field, such as fusion reactor, the back-scattering reaction cross section is known to become not negligible. Practically, until now, there were differences reported between experimental and calculated values of neutron benchmark experiments using a DT neutron source (deuterium-tritium), which focused on back-scattering phenomena like a gap streaming experiment to verify the prediction accuracy of neutron streaming passing through narrow gaps while scattering. For this problem, we developed a benchmark method for large-angle scattering cross sections and has carried out experiments to measure the large-angle elastic scattering cross section of iron for the last few years. The benchmark method was successfully established based on activation reaction of Nb having a large activation cross section at around 14 MeV. However, Nb foil takes a long time to obtain the enough number of counts due to the long half-life (10.2 day) and low detection efficiency of the decay gamma-ray. In this study, to find a more suitable activation foil, we examined possible nuclides having appropriately short half-lives, not so high gamma-ray energies because high detection efficiency is essential, large activation cross sections, and not too low threshold energies of nuclear reaction. The optimization was carried out by calculating and comparing the number of counts per reaction per nuclide for all nuclides listed in JENDL/AD-2017. As a result, we have found that $^{197}\text{Au}(n,2n)^{196}\text{Au}$ was the most suitable reaction giving us the largest number of counts in an acceptable short experimental time.

1. Introduction

As shown in Fig. 1, The neutron large-angles scattering reaction cross section data with high energy neutron. This difference is not negligible in neutronics designs of high neutron flux fields in such as fusion reactor. Therefore, it is necessary to measure back-scattering cross sections of Fe, Li, C, B etc. to be used in the fusion reactor design. For this problem we designed the experimental system to extract the contribution of large angle scattering reaction. [1] The benchmark method was successfully established based on the activation of Nb foil normally used to characterize DT neutron sources. [2] However, Nb foil takes a long time to obtain the enough number of counts due to the long half-life of about 10 days and the low detection efficiency of the decay gamma-ray (energy of the decay gamma-ray = 934 keV). In this study, to solve this problem, we examined possible activation nuclides having appropriately short half-lives, not so high decay gamma-ray energies because high detection efficiency is essential, large

cross sections. And not too low threshold energies are required for the accuracy of benchmark experiments.

2. Benchmark experiments

Basic structure of the experimental systems and neutron transport paths we consider in benchmark experiments are shown in Fig. 2. A shadow bar is installed to prevent neutrons from directly incident on activation foil, which detects neutrons, from a neutron source. Possible paths that a neutron can transport and contribute to the activation of the foil are numbered from 1 to 7. Path 1 is the neutron path via the shadow bar. Path 2 is the neutron path via the shadow bar and the sample. Path 3 is the backscattered neutron from the sample, which is an object to be extracted. Path 4 is the neutron path via the wall and shadow bar. Path 5 is the neutron path via the wall and the sample. Path 6 is the neutron path via the wall. Path 7 is the neutron path via the shadow bar and the wall and the sample.

The benchmark experiments are conducted in four experimental systems for extracting the contribution of large angle scattering reaction. Figure 3 shows the four experimental systems, two of which are with a thin shadow bar with and without the target, i.e., s1tc and s1c, and the rest two of which are with a thick shadow bar with and without the target, i.e., s2tc and s2c. Figure 3 also shows relation of the neutron transport paths that contribute to activation of the foil in each of the four systems. The contributions of paths 1, 4, and 6 are the same for s1tc and s1c, and for s2tc and s2c, because they depend on the size of the shadow bars, but not depend on that of the sample. That of path 5 is the same for s2tc and s1tc, and for s1c and s2c, because it depends on the presence of the sample. Therefore, calculating $s1tc-s2tc-(s1c-s2c)$, we can estimate the amount of activation by neutrons through paths 2, 3 and 7. Those of paths 2 and 7 does not cancel each other out. However, they are relatively a rare event, because the transporting neutron through the paths experiences a large number of scatterings. It means the contributions of paths 2 and 7 show less than path 3 largely. We thus regard the two contributions as the experimental error of the present benchmark method. By comparing the amount of activation obtained by the experiment with MCNP simulation (the Monte Carlo simulation) [3], the correctness of the backscattering cross section of the nuclear data can be verified. As an example, the result of a benchmark experiment with the iron sample is detailed in Ref. [2].

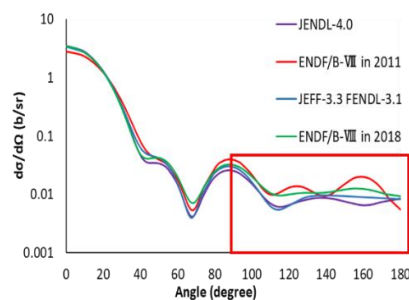


Figure 1 Angular distribution of neutron elastic scattering cross section of ^{56}Fe at 14 MeV. [4-8]

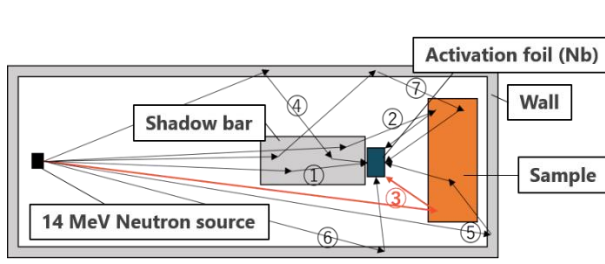


Figure 2 Basic structure of the experimental systems and neutron transport paths we consider in benchmark experiments. [1]

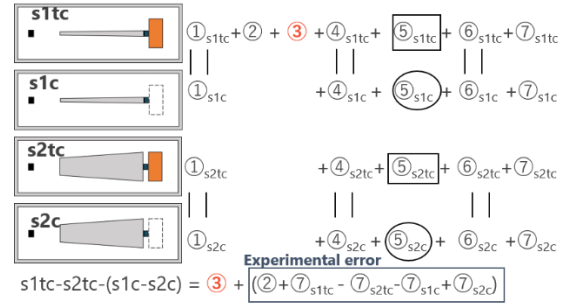


Figure 3 Four experimental systems and neutron transport paths that contribute to activation for each system. [1]

3. Method to optimize

At present, we need about one week to complete the benchmark experiments and another one week to finish measurement of the activation foils, in case of Nb foil is employed. To reduce the irradiation and measuring time, calculations of the number of counts for possible activation reactions were carried out for all nuclides stored in JENDL/AD-2017 using following equation:

$$\text{Count} = N \int_E \sigma f_n \varphi dE \times \frac{1}{\lambda} \times f \times g \times I_r \times \varepsilon \times (1 - e^{-\lambda t_i}) \times e^{-\lambda t_c} \times (1 - e^{-\lambda t_m}) \times DT \quad (1)$$

where N , σ , f_n , φ , λ , f , g , I_r , ε , t_i , t_c , t_m , DT represent the number of atoms, cross-section [cm^2] [9], factor of neutron self absorption [3], flux on foil calculated by MCNP with Fe sample [$\text{cm}^2/\text{source neutron}$], decay constant [1/s] [10], self shielding factor [11], isotopic ratio [12], gamma-ray emission ratio [10], gamma-ray detection efficiency, irradiation time [s], cooling time [s], measurement time [s] and neutron intensity [1/s] ($=5 \times 10^9$), respectively. Consequently, candidate activation nuclides showing the highest accuracy (the largest number of counts) were found. To prevent the error of the count number from being dominant, we searched for an activation foil that can obtain 10,000 counts in the shortest time.

Since the present benchmark experiments are conducted in OKTAVIAN facility of Osaka University, Japan, there are constraints on the present calculation as follows. The maximum irradiation time per day is 8 hours, and in the case of consecutive day's experiment, the cooling time of 16 hours between irradiations is required. In addition, the maximum measurement time was set to 5 days. And gamma-ray detection efficiency used the value when the decay gamma-rays are measured at a distance of 3.1 cm from the detection window using germanium detector. The energy of backscattered neutrons by the sample is about 8-14 MeV depending on kind of the sample nuclides, because the incident neutron energy is 14 MeV. Even if the reaction threshold energy is below 8 MeV, the reaction cross section may still be low for the backscattered neutrons. Therefore, in this study, we do not take into account the threshold energy, i.e., the threshold energy condition is set to 0-14 MeV.

4. Result

The number of counts of the decay gamma-ray from Nb foil and the one that can realize the count number larger than 2,000 counts in the combination of irradiation and measurement are shown in Fig. 4. This figure shows the increase in the number of counts measured for 1 to 5 days, when irradiation continues for 1 to 4 days. As can be seen from Fig. 4, it is found that the most efficient activation material

to obtain 10,000 counts for the shortest irradiation and experimental period is gold using $^{197}\text{Au}(n,2n)^{196}\text{Au}$ reaction. Table 1 shows a comparison of the threshold energy, cross-sectional area, half-life, gamma ray energy and gamma ray emission ratio of ^{196}Au and $^{92\text{m}}\text{Nb}$. However, since ^{196}Au has multiple excited state with a half-life of several minutes or more in Fig. 5 [13], it decays from two excited levels to the ground state over time. Then the number of counts of the decay gamma-ray from ground state is expected to be higher than estimation with Eq. (1).

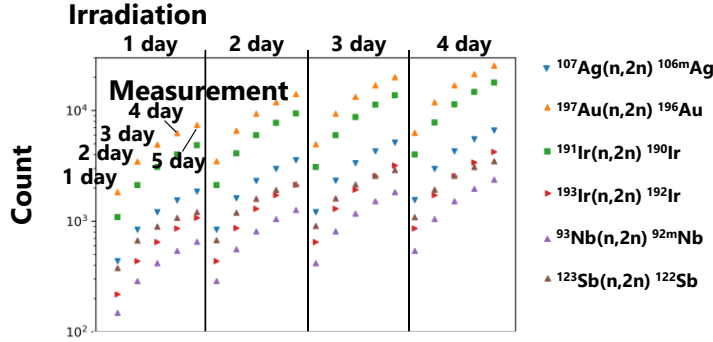


Figure 4 The number of counts of nuclides whose counts are larger than Nb foil.

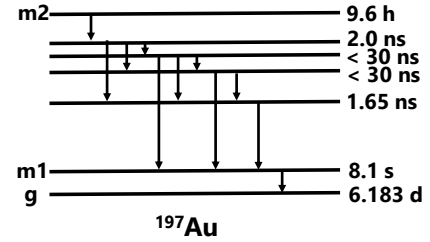


Figure 5 The multiple excited levels of ^{196}Au .

Table 1 Comparison of $^{92\text{m}}\text{Nb}$ and ^{196}Au .

	$^{92\text{m}}\text{Nb}$	$^{196\text{g}}\text{Au}$	$^{196\text{m1}}\text{Au}$	$^{196\text{m2}}\text{Au}$
Threshold energy [MeV]	9.1	8.1	8.2	8.7
Cross section at 14 MeV [barn] [8]	0.45	1.89	0.15	0.13
Half-life	10.1 d	6.1 d	8.1 s	9.6h
Energy of emitted gamma ray [keV]	934	356	85	148
Emission ratio [%]	99	87	0.3	43

5. Formulation of foil activation method using gold foil

If the number of counts is represented by Eq. (1), reaction rate, $\int_E \sigma \phi dE$, can be estimated from the number of counts of experiments. Then the correctness of the backscattering cross section of nuclear data can be verified by comparing the estimated reaction rate with the one calculated by the MCNP simulation. In the case of gold, the number of counts cannot be expressed simply by Eq. (1) with the fact described in Chap. 4. We thus need to formulate precisely to calculate the number of counts for gold in real applications. The number of counts in the case of two days of irradiation as shown in Fig. 6 is expressed by following equation:

$$\text{Count} = N_A \int_E R dE \times f \times g \times I_r \times \varepsilon, \quad (2)$$

where R is a term that includes cross section and decay constant, irradiation time, measurement time, and cooling time as shown in following equations. In these equations, σ_0 , σ_1 , σ_2 , λ_0 , λ_1 , λ_2 represent cross sections of ground state, first excited state, second excited state, decay constant of ground state, first excited state, second excited state, respectively.

$$R = (\varphi_2 A_2 + \varphi_1 B_2)(1 - e^{-\lambda_0 t_m}) + (\varphi_2 C_2 + \varphi_1 D_2) \left(1 - \frac{\lambda_2}{(\lambda_2 - \lambda_0)} e^{-\lambda_0 t_m} - \frac{\lambda_0}{(\lambda_2 - \lambda_0)} e^{-\lambda_2 t_m} \right) \quad (3)$$

$$\sigma = \frac{\sigma_0 + \sigma_1 + \sigma_2}{\lambda_0} + \frac{\sigma_1 + \sigma_2}{\lambda_1} + \frac{\sigma_2}{\lambda_2 - \lambda_0} \quad (4)$$

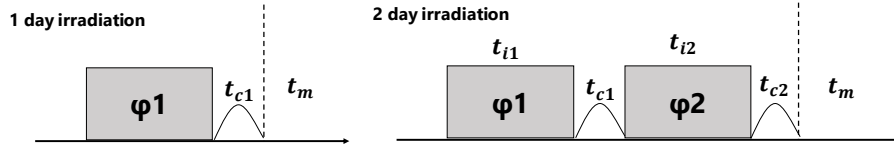


Fig. 6 Summary of the experiments.

For 1 day irradiation, irradiate with flux $\phi 1$ for t_{i1} , cool for t_{c1} and then measure the decay gamma-ray for t_m . For 2 day irradiation, irradiate with flux $\phi 1$ for t_{i1} , cool for t_{c1} and irradiate with flux $\phi 2$ for t_{i2} , cool for t_{c2} and then measure the decay gamma-ray for t_m .

where A, B, C and D are given as below:

$$\begin{aligned}
 A &= \sigma(1 - e^{-\lambda_0 t_{i1}}) + \frac{\sigma_2}{\lambda_0 - \lambda_2}(1 - e^{-\lambda_2 t_{i2}})e^{-\lambda_2 t_{c2}} + \frac{\sigma_2}{\lambda_1 - \lambda_2}(1 - e^{-\lambda_2 t_{i2}})e^{-\lambda_2 t_{c2}} \\
 &\quad + \frac{\sigma_2}{\lambda_2}(1 - e^{-\lambda_2 t_{i2}})e^{-\lambda_2 t_{c1}} + \frac{\sigma_2}{\lambda_1 - \lambda_2}(1 - e^{-\lambda_2 t_{i1}})e^{-\lambda_2 t_{c1} - \lambda_1 t_{i1}} \\
 B &= +\sigma(1 - e^{-\lambda_0 t_{i1}})e^{-\lambda_0 t_{i2}} + \frac{\sigma_2}{\lambda_0 - \lambda_2}(1 - e^{-\lambda_2 t_{i1}})e^{-\lambda_2 t_{c1} - \lambda_0 t_{i2}} \\
 &\quad + \frac{\sigma_2}{\lambda_0 - \lambda_2}(1 - e^{-\lambda_2 t_{i1}})e^{-\lambda_2(t_{i2} - t_{c1} - t_{c2})} + \frac{\sigma_2}{\lambda_1 - \lambda_2}(1 - e^{-\lambda_2 t_{i1}})e^{-\lambda_2(t_{c1} - t_{i2} - t_{c2})} \\
 C &= \frac{\sigma_2}{\lambda_2}(1 - e^{-\lambda_2 t_{i2}})e^{-\lambda_2 t_{c2}}, \quad D = \frac{\sigma_2}{\lambda_2}(1 - e^{-\lambda_2 t_{i1}})e^{-\lambda_2(t_{c1} - t_{i2} - t_{c2})}
 \end{aligned}$$

Recalculating the number of counts of $^{197}\text{Au}(n,2n)^{196}\text{Au}$ using Eq. (2), considering increment due to decay of $^{196m1}\text{Au}$ and $^{196m2}\text{Au}$, does not change significantly from Fig. 4 because σ_0 is one digit larger than σ_1 and σ_2 .

It is generally known that the nuclear data of the activation cross sections may have errors. Since the errors of nuclear data of the activation cross sections (σ_0 , σ_1 , σ_2) cause the errors of R calculated from MCNP simulation, it would be better to normalize σ_0 , σ_1 , σ_2 with accurate re-measured values at 14 MeV experimentally. Since the number of counts of gamma rays emitted from $^{196m2}\text{Au}$ can simply be calculated by Eq. (1), σ_2 can be normalized accurately at 14 MeV. On the other hand, since the emission ratio of gamma rays emitted from $^{196m1}\text{Au}$ is small, the half-life is very short and the number of $^{196m1}\text{Au}$ changes largely depending on the decay of $^{196m2}\text{Au}$, the number of counts of gamma rays emitted from $^{196m1}\text{Au}$ cannot be expressed by Eq. (1). As a result, σ_1 cannot be normalized easily. Similarly, the number of ^{196}Au changes irregularly due to existence of $^{196m1}\text{Au}$ and $^{196m2}\text{Au}$, σ_0 cannot also be normalized easily. Therefore, we consider the following measuring procedure to utilize $^{197}\text{Au}(n,2n)^{196}\text{Au}$ in benchmark experiments.

First of all, paying attention to the fact that R can be represented by σ_2 and σ (including σ_0 , σ_1 , and σ_2) as shown in Eqs. (3) and (4), it can be seen that normalizing only σ_2 and σ can eliminate the error of activation cross section in R. For normalizing σ , cooling for 3 days after 1day irradiation. Then $^{196m2}\text{Au}$ and $^{196m1}\text{Au}$ almost decay and finally fall to the state of ^{196}Au . Therefore, $^{197}\text{Au}(n,2n)^{196}\text{Au}$ can be regarded as the virtual reaction in which ^{196}Au is just generated with the cross section σ , and the count number can be calculated by following equation:

$$\text{Count} = N_A \int_E \phi_1 \sigma dE \times (1 - e^{-\lambda_0 t_{i1}})e^{-\lambda_0 t_{c1}} \times f \times g \times I_r \times \varepsilon \quad (5)$$

The virtual cross section value in Eq. (4), σ , can thus be normalized and to be used in real benchmark

experiments in future.

The experiment to measure σ_2 and σ precisely in OKTAVIAN facility of Osaka University is currently underway.

6. Conclusion

It was found from the theoretical examination that gold was the best activation foil to replace Nb foil for the present benchmark experiment. In addition, the difficulty of using the reaction of $^{197}\text{Au}(n,2n)$ due to the multiple excited levels, $^{196m1}\text{Au}$ and $^{196m2}\text{Au}$, in the activated gold foil is successfully overcome. After normalizing the cross section at 14 MeV at OKTAVIAN facility of Osaka University, the gold foil activation method would be utilized for our benchmark experiments in future.

References

- 1) Naoya Hayashi et al., "Optimization of Experimental System Design for Benchmarking of Large Angle Scattering Reaction Cross Section at 14MeV Using Two Shadow Bars", *Plasma and Fusion Research*, 2018; **13**: 2405002, 4p.
- 2) Atsuki Yamaguchi et al., "Benchmark experiment of large-angle scattering reaction cross section of iron at 14 MeV using two shadow bars – Comparison of experimental results with ENDF/B-VIII –", *Journal of Nuclear Science and Technology*, 58:1, 80-86 (2021). DOI: [10.1080/00223131.2020.1804475](https://doi.org/10.1080/00223131.2020.1804475)
- 3) Team, X-5 Monte Carlo, "MCNP –A General Monte Carlo N-Particle Transport Code, Version," Los Alamos National Laboratory, pp. LA-UR-03-1987, 2003.
- 4) K. Shibata et al., "JENDL-4.0: A New Library for Nuclear Science and Engineering," *J. Nucl. Sci. Technol.* 2011; **48(1)**: 1-30.
- 5) M.B. Chadwick et al., "ENDF/B-VII.0: Next Generation Evaluated Nuclear Data for Nuclear Science and Technology", *Nucl. Data Sheets*, 2006; **102**: 2931-3060.
- 6) JEFF-3.3 [Internet]. France: The Nuclear Energy Agency; 2017 Nov 20 [updated 2019 Aug. 2]. Available from: <https://www.oecd-nea.org/dbdata/jeff/jeff33/index.html>.
- 7) FENDL-3.1 [Internet]. Austria: International Atomic Energy Agency; 2016 July 1[2019 Aug. 2]. Available from: <https://www-nds.iaea.org/fendl/>.
- 8) D.A. Brown, M.B. Chadwick, R. Capote, et al., "ENDF/B-VIII.0: The 8th Major Release of the Nuclear Reaction Data Library with CIELO-project Cross Sections, New Standards and Thermal Scattering Data", *Nuclear Data Sheets*, 2018; **148**: 1-142.
- 9) Schemata, N.Iwamoto, S.Kunieda, F.Minato, O.Iwamoto "Activation Cross-section File for Decommissioning of LWRs" JAEA-Conf 2016-004, pp.47-52
- 10) S.Y.F. Chu, L.P. Ekström and R.B. Firestone, WWW Table of Radioactive Isotopes, database version 1999-02-28 from URL <http://nucleardata.nuclear.lu.se/nucleardata/toi/>
- 11) Berger, M.J., Hubbell, J.H., Seltzer, S.M., Chang, J., Coursey, J.S., Sukumar, R., Zucker, D.S., and Olsen, K. (2010), *XCOM: Photon Cross Section Database* (version 1.5). [Online] Available: <http://physics.nist.gov/xcom> [2020, 7, 10]. National Institute of Standards and Technology, Gaithersburg, MD.
- 12) Coursey, J.S., Schwab, D.J., Tsai, J.J., and Dragoset, R.A. (2015), *Atomic Weights and Isotopic Compositions* (version 4.1). [Online] Available: <http://physics.nist.gov/Comp> [2020, 5, 30]. National Institute of Standards and Technology, Gaithersburg, MD.
- 13) R. B. Firestone and C. M. Baglin, *Table of Isotopes*, 8th ed. (Wiley, New York, 1999).

(別紙)

14MeV 中性子による大角度弾性散乱反応断面積ベンチマーク実験のための放射化検出器の最適化

竹原峻平、福井和輝、荒木颯太、玉置慎吾、日下裕江、村田勲